# Optimal Thresholds for Differential Energy Detection of Ambient Backscatter Communication

Yuan Liu[1,2(✉)], Pinyi Ren[1,2], and Qinghe Du[1,2]

[1] School of Information and Communications Engineering, Xi'an Jiaotong University, Xi'an 710049, People's Republic of China
yuanaajy@163.com, {pyren,duqinghe}@mail.xjtu.edu.cn
[2] Shaanxi Smart Networks and Ubiquitous Access Research Center, Xi'an 710049, People's Republic of China

**Abstract.** With wide application of RFID, backscatter communication has become a focus in academy and industry. Specially, ambient backscatter communication has attracted much attention due to its low energy consumption and low cost. In this paper, we study the signal detection of the ambient backscatter communication system and focus on the differential energy detection method. Specifically, we use the off-the-shelf differential encoding model to eliminate the necessity of channel state information (CSI). Differential energy detection method and ML detector are applied as well to make the detecting results more precise and to obtain better performance. Based on them, we improve the approximate threshold and propose optimal thresholds decision algorithm of signal detection, which is proved feasible and efficient. Corresponding BER expressions are derived to estimate the performance of the algorithm. Simulation results are then provided to corroborate the theoretical studies. It can be shown from the results that using two optimal thresholds will improve the performance of the system to some extent, it will also be more tolerant to longer transmitting distance, especially when the channel status are not good.

**Keywords:** Ambient backscatter communication · Differential energy detection · Maximum likelihood (ML) detection · BER · Two optimal detection thresholds

## 1 Introduction

Radio frequency identification (RFID), one key technology for Internet of Things (IoT), attracts increasing intention in these years [1]. One typical RFID system consists of a reader and a tag [2]. The reader first generates an electromagnetic wave, the tag receives and backscatters the wave with modulated information bits to the reader [3]. The key communication pattern for RFID system is backscattering.

The research work reported in this paper is supported in part by the National Natural Science Foundation of China under the Grant No. 61941119 and Fundamental Research Funds for the Central Universities, China.


B. Li et al. (Eds.): IoTaaS 2020, LNICST 346, pp. 36–53, 2021.
https://doi.org/10.1007/978-3-030-67514-1_4

Backscatter communication can be divided into three types as in Fig. 1. The monastic backscatter is widely used in RFID and severe round-trip path loss of it will limit the communication distance between the reader and the tag [4–7]. To enlarge the transmitting area, bistatic backscatter technologies were proposed and a carrier emitter is added to the system to reduce the path loss of the signal, which performs better than traditional backscatter [8]. However, it is not always convenient to set an extra facility due to space and cost limit.

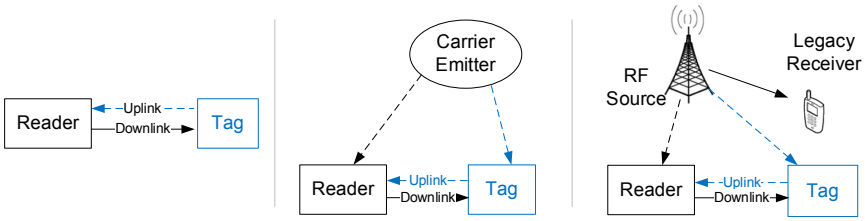


**Fig. 1.** Three categories in backscatter communication.

Ambient backscatter is a new type of backscatter communication which avoids the above shortcomings. The tags in ambient backscatter communication systems are battery-free devices powered by ambient radio frequency (RF) signals, e.g., wireless fidelity (Wi-Fi) and television (TV) radio. The tags are able to transmit 1 or 0 bit by switching the antenna impedance to reflect the ambient signals or not. After that, some algorithms will be utilized at the reader to detect the transmission status of the tag.

Even though ambient backscatter communication has grasped the intention, the signal processing and performance analysis for it is different from the existing communication and there exist many open problems worth further researching [9]. Several signal detection schemes for ambient backscatter communication systems and their performances are proposed in [10–12]. The ML detector with unknown channel state information (CSI) is presented in [10], it achieves the best performance but the complexity is too high. The joint-energy detector [11] employs the power of received signals in two consecutive intervals, which is simple to operate and requires only channel variances rather than specific CSI. To avoid the estimation of the channel parameters, applying the differentiate energy detector is a good choice. [12] proposes this method and exploits the differences between signal powers in two consecutive intervals, which does not need CSI and training symbols.

In this very work, we focus on the differentiate energy detection and BER performance at the reader. To improve the performance of the detector, we aim to improve the accuracy of the detecting threshold and reanalyze it in mathematical form. We derivate that in most cases, there will be two optimal thresholds. As a consequence, new decision standard is developed. BER performance is an essential indicator in evaluating the ambient backscatter communication system, so to validate the efficiency of our standard, the BER expression is derived and analyzed. Finally, numerical simulation results are provided to verify that optimal thresholds will provide better BER performance, be more tolerant to long distances and reduce the complexity, especially when the channel status are not good.

The rest of this paper is organized as follows: Sect. 2 depicts the theoretical model for ambient backscatter communication systems. Section 3 derives the ML detector using the differentiate power and an approximate decision threshold, obtaining corresponding decision region. Section 4 gives optimal thresholds decision algorithm in different scenarios and analyzes the connections between BER performance and parameters. The improvement is also presented. Simulations and results are shown in Sect. 5 and Sect. 6 concludes the paper.

## 2 System Model

Ambient backscatter communication system is easy to describe since it has a simple structure composed by one reader, one tag and a RF source, this RF source will emit RF signals such as TV signals, Wi-Fi signals and cellular transmissions. The tag in the system modulates this signal and backscatters the processed signal to the reader. Then the detection process begins at the reader.

We assume that RF signal is expressed as $s(n)$, which is the complex baseband equivalent signal and obeys BPSK modulation. Tag receives the RF signal and transmits its own binary signal $B(k)$ to the reader through choosing whether to backscatter $s(n)$ or not. Here we also suppose that the data rate of $B(k)$ is much less than that of $s(n)$. Quantitatively, in one data interval of $B(k)$, the RF source will send out $N$ RF signals.

Tag is a passive device and it will switch its impedance inside its circuit to decide the backscatter state. Specifically, if $B(k) = 0$, little energy of $s(n)$ is reflected. While if $B(k) = 1$, the tag will reflect the whole signal to the reader.

Since we focus most on the backscattered signal from the tag, the final detection is about $B(k)$. However, due to the randomness of the wireless channel, it is hard to get CSI and carry out signal detection with it. At the same time, in order to avoid power-consuming and complexity-increasing training sequences for the battery-free tag operation [13, 14], and also to avoid the high BER at the reader with blind detector [15], we derive an off-the-shelf differential encoding model from [12] at the tag to do some processing in advance. The differential encoding is realized by a differential encoder before the modulator and the model is shown in Fig. 2. Where $A(k)$ is the input and $B(k)$ is the output. They have mathematical connections as

$$B(k) = A(k) \otimes B(k-1), \tag{1}$$

where $\otimes$ represents addition modulo 2.

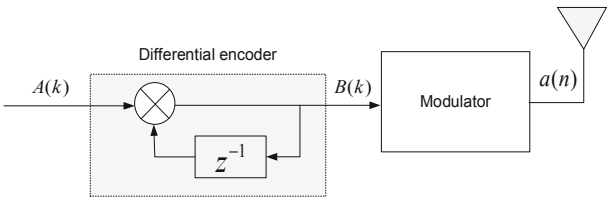


**Fig. 2.** Differential encoding model.

From the expression, it is easy to get that $A(k)$ stands for the changing-or-not situation of $B(k)$ in two consecutive time intervals: bit "0" for $A(k)$ corresponds to the same states in two intervals before and after, while bit "1" corresponds to the transition from two status. With this model, we will use the detection of $A(k)$ to replace that of $B(k)$ to lower the complexity.

Also, for convenience, we denote the channel between the RF source and the reader as $h$, the channel between the RF source and the tag as $g$ and the channel between the reader and the tag as $\zeta$. The model is presented in Fig. 3. They are all assumed as slow-fading and will remain unchanged during at least two consecutive intervals of $B(k)$. Furthermore, all these channels are unknown to the reader.

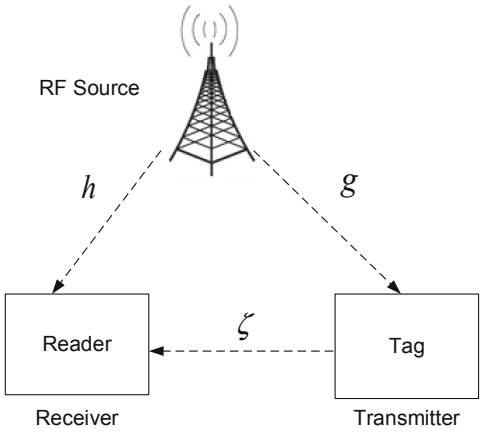


**Fig. 3.** Channel model of ambient backscatter communication.

With these denotation, we can express the signals sent or received at three devices. Knowing the RF signal is $s(n)$, then the tag receives the transmitted signal

$$x(n) = gs(n). \tag{2}$$

And the signal backscattered by the tag can be expressed as

$$a(n) = \eta B(k)x(n), B(k) \in \{0, 1\} \tag{3}$$

where $\eta$ is the complex signal attenuation inside the tag. Since the data rate of the RF signal $s(n)$ is $N$ times of that of $B(k)$, $B(k)$ will remain unchanged within $N$ symbols of $x(n)$.

Thus, the passband signal received by the reader is

$$y(n) = hs(n) + \zeta a(n) + w_b(n), \tag{4}$$

where $w_b(n)$ is the zero-mean additive white Gaussian noise (AWGN) with variance $N_{wb}$.

Though the backscattered signal is superposed on ambient signals at the reader, only the status of reflecting or non-reflecting is aimed to be detected [16], so we have to recover $B(k)$ from the received signal $y(n)$ in case of no CSI knowledge. Note that the ambient backscatter communication system differs from traditional communication systems in that $B(k)$ is hidden in $y(n)$. Consequently, the previous detection methods used in traditional communication systems become invalid and a new detection method must be designed to recover $B(k), k = 1, 2, \cdots K$.

Before the design and implementation of new method, we give some remarks to get a better understanding.

*Remark 1:* Since the inserted integrated circuit of the tag considered in the ambient backscatter system only consists of passive components and involves at most no signal processing operation, the thermal noise at the tag is normally omitted [17].

*Remark 2:* Strictly speaking, there exists a time delay $\tau$ between the arriving time of $s(n)$ and $a(n)$ at the reader. However, such a delay can be ignored because the communication range among RF-powered devices is limited and the transmission speed of electrical signals inside the on-tag integrated circuit are as fast as light speed [8], the transmitting time is very short.

## 3 Received Signal Detection

### 3.1 Format of the Signal

In the former section, we have known that $B(k)$ can be 0 or 1 according to its impedance state. Based on this, we can rewrite the expression of received signal $y(n)$ as

$$y(n) = \begin{cases} hs(n) + \omega_b(n), & B(k) = 0, \\ \mu s(n) + \omega_b(n), & B(k) = 1, \end{cases} \tag{5}$$

where $\mu \triangleq h + \eta\zeta g$ denotes the combined channel information.

In the next step, to detect the signal with differentiate energy, the power of the signals is to be derived. Here we suppose that the tag transmits $K$ symbols in the whole transmitting process so that the reader receives $KN$ signals in total and these signals can be divided into $K$ groups corresponding to $K$ $B(k)$ s. Each group consists of $N$ signals and we compute the average power of them as

$$\Gamma_k = \frac{1}{N} \sum_{n=(k-1)N+1}^{kN} |y(n)|^2, \ 1 \le k \le K \tag{6}$$

Based on the expression of $y(n)$, we can easily decompose $\Gamma_k$ and get the distribution of it in different cases [12]

When $N$ is large,

$$\Gamma_k = \begin{cases} \Gamma_{k,0} \sim \mathcal{N}(|h|^2 P_s + N_{\omega b}, \varsigma_0^2), \\ \Gamma_{k,1} \sim \mathcal{N}(|\mu|^2 P_s + N_{\omega b}, \varsigma_1^2). \end{cases} \tag{7}$$

When $N$ is small,

$$\Gamma_k = \begin{cases} \Gamma_{k,0} \sim \mathcal{N}(|h|^2 P_s + N_{\omega b}, \sigma_0^2), \\ \Gamma_{k,1} \sim \mathcal{N}(|\mu|^2 P_s + N_{\omega b}, \sigma_1^2). \end{cases} \tag{8}$$

where

$$\varsigma_0^2 = \frac{2}{N}|h|^2 P_s N_{wb}, \varsigma_1^2 = \frac{2}{N}|\mu|^2 P_s N_{wb}, \sigma_0^2 = \frac{N_{wb}^2}{N} + \varsigma_0^2, \sigma_1^2 = \frac{N_{wb}^2}{N} + \varsigma_1^2, \tag{9}$$

where $P_s$ is the average power of $s(n)$ and is unknown to the reader.

For the simplicity, we take the first case as an example to analyze the detection process and performance, the corresponding discussions for small $N$ case can be similarly obtained [12].

### 3.2 ML Detection

We have mentioned the reason for deriving the differentiate encoding in the former section. By using it, the detection of $B(k)$ is transformed into that of $A(k)$, which implies the change of tag signal. This transformation fits the model properly and it can also be reflected in the power change of the received signal at the reader during two transmitting intervals of $B(k)$. So in this paper, we utilize the power difference $\Phi_k$ to detect the signal, i.e., to obtain $A(k).\Phi_k$ has the following expression

$$\Phi_k = \Gamma_k - \Gamma_{k-1}. \tag{10}$$

The optimal detector should minimize the error probability, which means that the correct probability should be maximized as much as possible by using this detector, i.e.,

$$\begin{aligned} \hat{A}(k) &= \arg \max_{A(k)\in[0,1]} \Pr(\text{correct decision}|\Phi_k) \\ &= \arg \max_{A(k)\in[0,1]} \Pr(A(k)|\Phi_k). \end{aligned} \tag{11}$$

According to Bayes' rule and the fact that $A(k) = 0$ and $A(k) = 1$ are equal-probable, we will write (11) as

$$\hat{A}(k) = \arg \max_{A(k)\in[0,1]} \Pr(\Phi_k|A(k)). \tag{12}$$

The detectors (12) is well-known as a maximum likelihood (ML) detector.

### 3.3 Approximate ML Decision Region

Since the tag uses differential encoding, $A(k)$ can be fully determined by $B(k)$ and $B(k-1)$. Based on the distribution of $\Gamma_k$, the distribution of $\Phi_k$ can be easily checked: $\Phi_{k|0,0} \sim \mathcal{N}(0, 2\varsigma_0^2)$, $\Phi_{k|1,1} \sim \mathcal{N}(0, 2\varsigma_1^2)$, $\Phi_{k|0,1} \sim \mathcal{N}(\delta, \varsigma_0^2 + \varsigma_1^2)$ and $\Phi_{k|1,1} \sim \mathcal{N}(-\delta, \varsigma_0^2 + \varsigma_1^2)$, where the subscript of $\Phi_k$ represents different combination of $B(k)$ and $B(k-1)$.

Note that

$$\delta = (|\mu|^2 - |h|^2)\mathrm{P}_s. \tag{13}$$

Let $p(\Phi_{k|0,0})$, $p(\Phi_{k|1,1})$, $p(\Phi_{k|0,1})$ and $p(\Phi_{k|1,0})$ denote the probability density functions (PDFs) of the conditional Gaussian distributed random variables above.

We define

$$p_0(x) = \Pr(\Phi_k | A(k) = 0), \tag{14}$$

$$p_1(x) = \Pr(\Phi_k | A(k) = 1), \tag{15}$$

which can be expressed further as

$$p_0(x) = \frac{1}{2}\left((p(\Phi_{k|0,0}) + p(\Phi_{k|1,1})\right) = \frac{1}{4\sqrt{\pi\varsigma_0^2}} e^{-\frac{x^2}{4\varsigma_0^2}} + \frac{1}{4\sqrt{\pi\varsigma_1^2}} e^{-\frac{x^2}{4\varsigma_1^2}}, \tag{16}$$

$$p_1(x) = \frac{1}{2}\left((p(\Phi_{k|0,1}) + p(\Phi_{k|1,0})\right) = \frac{1}{\sqrt{8\pi\varsigma_+^2}} e^{-\frac{(x-\delta)^2}{2\varsigma_+^2}} + \frac{1}{\sqrt{8\pi\varsigma_+^2}} e^{-\frac{(x+\delta)^2}{2\varsigma_+^2}}, \tag{17}$$

where

$$\varsigma_+^2 = \varsigma_0^2 + \varsigma_1^2. \tag{18}$$

Subsequently, ML detection rule can be reformulated as

$$\begin{cases} \hat{A}(k) = 0, p_0(x) > p_1(x), \\ \hat{A}(k) = 1, p_0(x) < p_1(x). \end{cases} \tag{19}$$

To clearly distribute the decision region, we have to obtain the decision threshold $Th$. The detected results in the left and right region of threshold $Th$ are opposite, while the following condition should be satisfied at threshold $Th$

$$p_0(x) = p_1(x)|_{x=Th}. \tag{20}$$

From the known formulas, this equation has a complex form and does not have a closed-form solution. However, we have two ways to obtain the threshold $Th$. Firstly, we resort to obtain an approximate solution to replace it; secondly, some approximation methods in certain ranges will be applied to approach the optimal solution. Here we talk about the first method and another one will be discussed in detail in the next section.

We define the approximate threshold as $Th^{apx}$, which satisfies (30). Assume that $\delta$ is very small and $\varsigma_1 = \varsigma_0$, then the following approximation is obtained

$$\tilde{p}_0(x) = \frac{1}{2}((p(\Phi_{k|0,0}) + p(\Phi_{k|1,1})) = \frac{1}{\sqrt{2\pi\varsigma_+^2}} e^{-\frac{x^2}{2\varsigma_+^2}}, \tag{21}$$

$$\tilde{p}_1(x) = \frac{1}{2}((p(\Phi_{k|0,1}) + p(\Phi_{k|1,0})) = \frac{1}{\sqrt{8\pi\varsigma_+^2}} e^{-\frac{(x-\delta)^2}{2\varsigma_+^2}} + \frac{1}{\sqrt{8\pi\varsigma_+^2}} e^{-\frac{(x+\delta)^2}{2\varsigma_+^2}}. \tag{22}$$

Replacing the two terms in (20) with (21) and (22), we obtain

$$T_h^{apx} = \frac{|\delta|}{2} + \frac{\varsigma_+^2}{|\delta|} \ln(1 + \sqrt{1 - e^{-\delta^2/\varsigma_+^2}}). \tag{23}$$

With this approximate threshold, the decision region can be described as

$$\begin{cases} \hat{A}(k) = 0, |\Phi_k| < |Th^{apx}|, \\ \hat{A}(k) = 1, |\Phi_k| > |Th^{apx}|. \end{cases} \tag{24}$$

# 4 Optimal Thresholds for Detection

## 4.1 Different Scenarios

In the last section, we have obtained the approximate threshold under the assumption $\varsigma_1 = \varsigma_0$. However, in actual situation, they will not be equal at most of the time, which means there always exist differences between channels. So to make the threshold more robust and be widely applied in all scenarios, we optimize the approximate threshold and obtain an optimal threshold decision algorithm.

To be concrete, when $\delta < \varsigma_+$, we do analysis for $p_0(x)$ and $p_1(x)$: when $x = 0$, $p_0(x) > p_1(x)$ and when $x \to \infty$, $p_0(x) > p_1(x)$, knowing that $p_0(x)$ and $p_1(x)$ are both decreasing in $(0, +\infty)$, we can get the conclusion that they at least have two intersection points, thus two thresholds are obtained in $(0, +\infty)$. According to the relative value of $\delta$ and $\varsigma_+$, three situations are summarized in Fig. 4 and we find their corresponding two optimal thresholds $Th^{opt1}$ and $Th^{opt2}$ respectively.

**Case 1:** $\delta < \varsigma_+$. In this case, it is clear that both $p_0(x)$ and $p_1(x)$ have only one peak. Thus to get the thresholds, we just have to obtain the intersection points of two PDFs. Since the closed-form solutions are unavailable, we use piecewise dichotomy to approach the solutions. In this method, the determination of demarcation point is very essential and at this point, condition $f(x) = p_0(x) - p_1(x) < 0$ should be satisfied. To get this point, we first consider $Th^{apx}$ and estimate whether it could be the demarcation point. If it satisfies the condition, $(0, +\infty)$ will be divided into two segments:$(0, Th^{apx})$ and $(Th^{apx}, +\infty)$. Then we use dichotomy to get the optimal solutions. If the condition cannot be satisfied at

$Th^{apx}$, we would rather consider another point $Th^{dem}$ and estimate the feasibility to choose it as the demarcation point in the same way. $Th^{dem}$ is computed as

$$Th^{dem} = \frac{2\varsigma_+^2 \ln 2 + \delta^2}{2\delta}. \tag{25}$$

If condition $f(x) < 0$ is not reached at any point, it will be difficult to get the optimal thresholds and we resort to replace them with $Th^{opt1} = Th^{apx}$ and $Th^{opt2} = +\infty$.

*Remark 3:* $Th^{dem}$ is obtained from equation $p_0(x) = p(\Phi_{k|0,1})|_{x=Th^{dem}}$ under the condition $\varsigma_1 = \varsigma_0$. Since $p(\Phi_{k|1,0})$ is decreasing in $(0, +\infty)$ and it plays a less important role in determining the value of $p_1(x)$, we omit it and just take $p(\Phi_{k|0,1})$ into consideration to find a threshold.

**Case 2:** $\delta > \varsigma_+$ and value of $\delta$ is moderate. In this case, there are two peaks for $p_1(x)$ in range $(-\delta, \delta)$, the proof is shown in Appendix. As Fig. 4 shows, when the value of $\delta$ is modest, the two peaks are at the outside of the peak of $p_0(x)$, $f(x) < 0$ is satisfied at most time when $x = \delta$. At this time, $\delta$ can be a demarcation point and then we will obtain two optimal thresholds. However, when it happens that $f(x) > 0$ when $x = \delta$, $Th^{apx}$ and $Th^{dem}$ will be evaluated to be the demarcation point as described in Case 1.

**Case 3:** $\delta > \varsigma_+$ and the value of $\delta$ is very small. Two peaks of $p_1(x)$ are within the peak of $p_0(x)$. The peak of $p_1(x)$ in $(0, +\infty)$ is on the left of $x = \delta$, so we do not know the exact position of $\delta$ and whether the demarcation point condition will be satisfied. Thus it is necessary to discuss the positive and negative of $f(x)$ when $x = \delta$. If $x = \delta$ can not be a demarcation point, to get the solution in this case, we make comparison with Case 1 and find that two cases are similar to each other, so the steps in Case 1 are repeated to help us find two optimal thresholds.

Above all, Case 2 and Case 3 both belong to the case $\delta > \varsigma_+$. In this situation, we just have to i) Judge that whether $x = \delta$ will be used to divide the range. ii) If so, use dichotomy to find two optimal thresholds. iii) If not, repeat steps in case 1 to obtain the solutions.

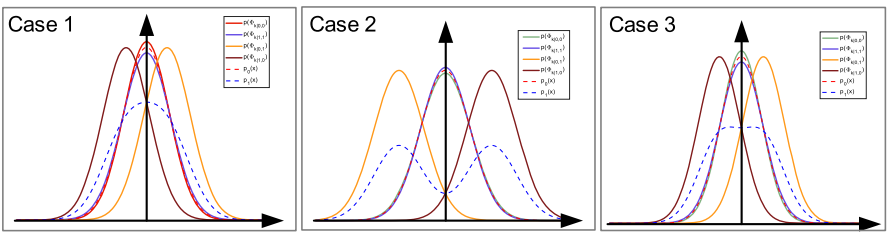


**Fig. 4.** PDFs of $\Phi_{k|0,0}$, $\Phi_{k|1,1}$, $\Phi_{k|0,1}$, $\Phi_{k|1,0}$ and their combination $p_0(x)$, $p_1(x)$ in three cases.

### 4.2 Optimal Thresholds Decision Algorithm

To summarize, we discover that $\delta$ plays a vital role in distinguishing three cases and determining the segmentation point. When $\delta > \varsigma_+$ and $\delta$ is moderate, it is very likely

to be chosen as the segmentation point and two thresholds will be in its left and right range. However, when it is too small, it may not be a good choice for dividing two segments. We resort to analyze $Th^{apx}$ and $Th^{dem}$ then obtain the solutions. The algorithm is shown in the following table:

**Algorithm 1 Optimal Thresholds Decision**

**Input:** $\delta$、$\varsigma_0$、$\varsigma_1$

**Output: Optimal thresholds** $Th^{opt1}$ **and** $Th^{opt2}$

**Case 1:** $\delta < \varsigma_+$
Compute $f(x)|_{x=Th^{apx}}$.
**if** $f(x)|_{x=Th^{apx}} < 0$ **then**
use dichotomy in $(0, Th^{apx})$ and $(Th^{apx}, +\infty)$, obtain $Th^{opt1}$ and $Th^{opt2}$.
**else**
compute $f(x)|_{x=Th^{dem}}$.
**if** $f(x)|_{x=Th^{dem}} < 0$ **then**
use dichotomy in $(0, Th^{dem})$ and $(Th^{dem}, +\infty)$, obtain $Th^{opt1}$ and $Th^{opt2}$.
**else**
$Th^{opt1} = Th^{apx}$, $Th^{opt2} = +\infty$.
**end if**
**end if**
**Case 2:** $\delta < \varsigma_+$
Compute $f(x)|_{x=\delta}$.
**if** $f(x)|_{x=\delta} < 0$ **then**
use dichotomy in $(0, \delta)$ and $(\delta, +\infty)$, obtain $Th^{opt1}$ and $Th^{opt2}$.
**else**
compute $f(x)|_{x=Th^{apx}}$.
**if** $f(x)|_{x=Th^{apx}} < 0$ **then**
use dichotomy in $(0, Th^{apx})$ and $(Th^{apx}, +\infty)$, obtain $Th^{opt1}$ and $Th^{opt2}$.
**else**
compute $f(x)|_{x=Th^{dem}}$.
**if** $f(x)|_{x=Th^{dem}} < 0$ **then**
use dichotomy in $(0, Th^{dem})$ and $(Th^{dem}, +\infty)$, obtain $Th^{opt1}$ and $Th^{opt2}$.
**else**
$Th^{opt1} = Th^{apx}$, $Th^{opt2} = +\infty$.
**end if**
**end if**
**end if**

Based on the algorithm, the decision regions are shown below

$$\begin{cases} \hat{A}(k) = 0, |\Phi_k| < \left|Th^{opt1}\right| or |\Phi_k| > \left|Th^{opt2}\right|, \\ \hat{A}(k) = 1, \left|Th^{opt1}\right| < |\Phi_k| < \left|Th^{opt2}\right|. \end{cases} \tag{26}$$

### 4.3 BER Performance

BER is an important metric to evaluate the performance of system, so here we derive the expression of it to show the connections of BER and parameters clearly.

The BER for the aforementioned ML detector is obtained from

$$\begin{aligned} P_b &= \Pr(A(k) = 1) \Pr(\hat{A}(k) = 0 | A(k) = 1) + \Pr(A(k) = 0) \Pr(\hat{A}(k) = 1 | A(k) = 0) \\ &= \frac{1}{2}(\frac{1}{2} P_{b|0,0} + \frac{1}{2} P_{b|1,1}) + \frac{1}{2}(\frac{1}{2} P_{b|0,1} + \frac{1}{2} P_{b|1,0}). \end{aligned} \tag{27}$$

where $P_{b|0,0}$ and $P_{b|1,1}$ are obtained by using optimal detecting thresholds and the Gaussian tail probability Q function

$$\begin{aligned} P_{b|0,0} &= \Pr(\hat{A}(k) = 1 | B(k-1) = 0, B(k) = 0) \\ &= 2 \int_{Th^{opt1}}^{Th^{opt2}} p(\Phi_{k|0,0}) d\Phi_{k|0,0} = 2(Q(\frac{Th^{opt1}}{\sqrt{2\varsigma_0^2}}) - Q(\frac{Th^{opt2}}{\sqrt{2\varsigma_0^2}})), \end{aligned} \tag{28}$$

$$\begin{aligned} P_{b|1,1} &= \Pr(\hat{A}(k) = 1 | B(k-1) = 1, B(k) = 1) \\ &= 2 \int_{Th^{opt1}}^{Th^{opt2}} p(\Phi_{k|1,1}) d\Phi_{k|1,1} = 2(Q(\frac{Th^{opt1}}{\sqrt{2\varsigma_1^2}}) - Q(\frac{Th^{opt2}}{\sqrt{2\varsigma_1^2}})). \end{aligned} \tag{29}$$

Actually, $P_{b|0,1} = P_{b|1,0}$ due to symmetry

$$\begin{aligned} P_{b|0,1} = P_{b|1,0} &= \Pr(\hat{A}(k) = 0 | B(k-1) = 1, B(k) = 0) \\ &= 1 - 2 \int_{Th^{opt1}}^{Th^{opt2}} p(\Phi_{k|1,0}) d\Phi_{k|1,0} = 1 - 2(Q(\frac{Th^{opt1} + \delta}{\sqrt{\varsigma_0^2 + \varsigma_1^2}}) - Q(\frac{Th^{opt2} + \delta}{\sqrt{\varsigma_0^2 + \varsigma_1^2}})), \end{aligned} \tag{30}$$

where

$$Q(x) = \frac{1}{\sqrt{2\pi}} \int_x^{\infty} e^{-\frac{t^2}{2}} dt. \tag{31}$$

Therefore, substituting (28), (29) and (30) into (27), we finally obtain the BER expression as

$$\begin{aligned} P_b = & \frac{1}{2}\left(Q\left(\frac{Th^{opt1}}{\sqrt{2\varsigma_0^2}}\right) + Q\left(\frac{Th^{opt1}}{\sqrt{2\varsigma_1^2}}\right)\right) - \frac{1}{2}\left(Q\left(\frac{Th^{opt2}}{\sqrt{2\varsigma_0^2}}\right) + Q\left(\frac{Th^{opt2}}{\sqrt{2\varsigma_1^2}}\right)\right) \\ & + \frac{1}{2}\left(1 - 2\left(Q\left(\frac{Th^{opt1} + \delta}{\sqrt{\varsigma_0^2 + \varsigma_1^2}}\right) - Q\left(\frac{Th^{opt2} + \delta}{\sqrt{\varsigma_0^2 + \varsigma_1^2}}\right)\right)\right). \end{aligned} \tag{32}$$

Although BER performance appears different under different thresholds, they have the same trend and connection with parameters, so here we use approximation thresholds under high SNR: $Th^{opt1} = |\delta|/2$ and $Th^{opt2} = +\infty$ to analyze.

*Proof:* Since

$$T_h^{apx} = \frac{|\delta|}{2} + \frac{\varsigma_+^2}{|\delta|}\ln\left(1 + \sqrt{1 - e^{-\delta^2/\varsigma_+^2}}\right). \tag{33}$$

When it is in high SNR, the second term of $Th^{apx}$ is much smaller than the first one, thus can be omitted. So we obtain

$$Th^{opt1} = \frac{|\delta|}{2}, Th^{opt2} = +\infty. \tag{34}$$

Substitute (34) into (32), then we get BER expression as

$$\begin{aligned} P_b = & \frac{1}{2}Q\left(\frac{\Delta_{\mu h}}{4|h|}\sqrt{\gamma N}\right) + \frac{1}{2}Q\left(\frac{\Delta_{\mu h}}{4|\mu|}\sqrt{\gamma N}\right) \\ & + \frac{1}{2}Q\left(\frac{\Delta_{\mu h}}{2\sqrt{2}\sqrt{\Xi_{\mu h}}}\sqrt{\gamma N}\right) - \frac{1}{2}Q\left(\frac{3\Delta_{\mu h}}{2\sqrt{2}\sqrt{\Xi_{\mu h}}}\sqrt{\gamma N}\right), \end{aligned} \tag{35}$$

where $\gamma = \mathrm{P}_s/N_{\omega b}$ and $\Delta_{\mu h} = \left||\mu|^2 - |h|^2\right|$, $\Xi_{\mu h} = |\mu|^2 + |h|^2$.

From this new expression, we can conclude that in ambient backscatter communication system, BER is not only determined by the SNR and channel fading as in traditional communication system, but also by the channel difference $\Delta_{\mu h}$ and the RF signal number $N$ in one group.

### 4.4 Improvement Analysis

The essence of signal detection is to divide the decision area into different sections. By analysis, we found that the whole decision range is divided into five segments by our two optimal thresholds, in two of them, signals are decided as $A(k) = 1$ while in the other three, signals are detected as $A(k) = 0$. Compared with the previous method

which divides three parts, this new algorithm will make detection results more accurate. Especially, when the obtained two thresholds are close to each other, the five segments are more clearly presented and using the earlier detecting threshold will cause mistakes easily if the observed power difference lays in the outside range of $Th^{opt2}$. So in this case, our optimal two thresholds have a lot to do to decrease BER. In contrast, if two thresholds are very far from each other, it is hard for the power difference to exceed $Th^{opt2}$, and divided five parts are not so apparent that the significance of our algorithm is just making $Th^{opt1}$ closer to its true value. The improvement exists but is not as great as the former one. The simulation results will testify our analysis in the next section.

## 5 Simulations and Results

In this section, we resort to numerical examples to evaluate the proposed studies. In our simulations, the noise variance $N_{wb}$ is set as 1 and $K$ is chosen as 100. Since the distance between RF source and tag (or reader) is much larger than that between tag and reader, we generate $h$ and $g$ according to $\mathcal{CN}(0,1)$ and generate $\zeta$ according to $\mathcal{CN}(0,10)$ at the beginning. Energies of all channels are assumed to hold unchanged during $K$ $B(k)$ s' symbols period. The complex signal attenuation $\eta$ inside the tag is fixed as 1.1 dB [18]. In order to include as many situations as possible, we do $10^5$ Monte Carlo simulations in total.

It need to be mentioned that, to use the received data for detection and avoid training symbols for channel estimation, we can also use $E(|\Phi_k|)$ as an approximation threshold, it also approaches $|\delta|/2$ when $K$ is relatively large. It can be expressed as

$$E(|\Phi_k|) \approx \frac{1}{K}\sum_{k=1}^{K}|\Phi_k|. \tag{36}$$

Figure 5 shows the trend of BER under three different thresholds: $Th^{opt1}\&Th^{opt2}$,$Th^{apx}$ and $E(|\Phi_k|)$, with SNR ranging from 5 to 30 dB. Threshold $E(|\Phi_k|)$ is obtained from calculation of power difference and the other two thresholds are the results of algorithm and formula we derived. The number of signals $N$ that RF source sends in one time interval of $B(k)$ is set to be 20 and 50 for comparison. For each SNR, $\Phi_k$ is divided into different ranges by thresholds and the signal is detected, then we get corresponding BER. It can be shown that as SNR increases, BER goes down whichever threshold is used. BER performances are similar when using $Th^{apx}$ and $E(|\Phi_k|)$ as the single threshold. However, when two thresholds $Th^{opt1}$ and $Th^{opt2}$ are taken into consideration, there is an apparent decrease in BER due to the accuracy and completeness of the decision threshold. It is also found that larger $N$ will reduce BER to some degree.

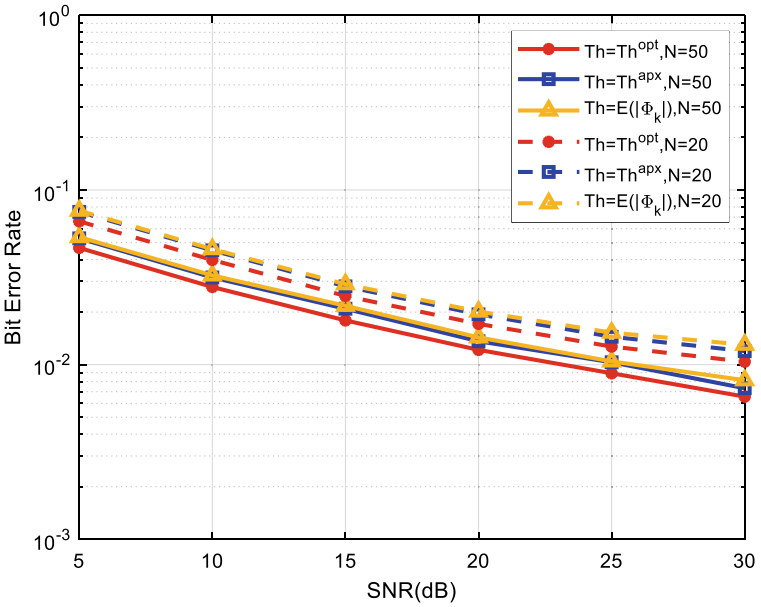


**Fig. 5.** BER versus transmit SNR under different thresholds and $N$.

In Fig. 6, we change the channel status by changing the variance of $h$, $g$ and $\zeta$ to 0.1,0.1 and 1, respectively. It means that channel status turn poor. $N$ is fixed as 50. What is clearly observed is that BER has an increase due to the poor channel quality.

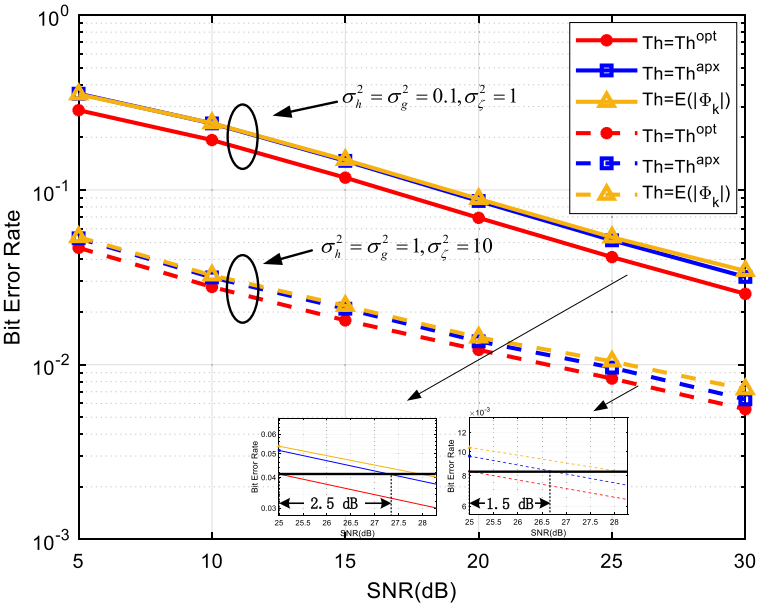


**Fig. 6.** BER performance improvement in two channel status.

On the other hand, not surprisingly, the result meets our analysis. In this situation, BER performance has a great improvement compared with that in the former case. When the channel status is stable, there is an approximate 1.5 dB improvement, while it has an improvement of about 2.5 dB in average when channel quality is worsened. This is because when the channel status are not good, two optimal thresholds are close to each other, then the detecting results will have great changes, especially when $|\Phi_k| > \left|Th^{opt2}\right|$. Results show that our algorithm will provide better performance especially in poor channel status, making the system have strong tolerance to longer distances and obstacles in transmitting path.

Figure 7 shows the curves of BER versus $N$ under three thresholds when SNR = 30 dB. Corresponding BERs are plotted. Clearly, BER decreases as $N$ increases under each threshold. We can also observe from the figure that when $N$ is small, the decreasing trend is very quick, whereas it slows down when $N$ is large and BER curve will tend to be flat when $N$ is larger than 140 or so. This enlightens us to consider the complexity of detection since $N$ is related to the computational complexity. Specifically, it is better to choose a modest $N$ to achieve good BER performance. What is also shown in Fig. 7 is that our two thresholds algorithm greatly improves the performance of the system. When $N$ and SNR are determined, using two optimal thresholds results in lowest BER compared with other thresholds, meanwhile, with the same BER, less RF signals will be sent, thus the computational complexity is reduced.

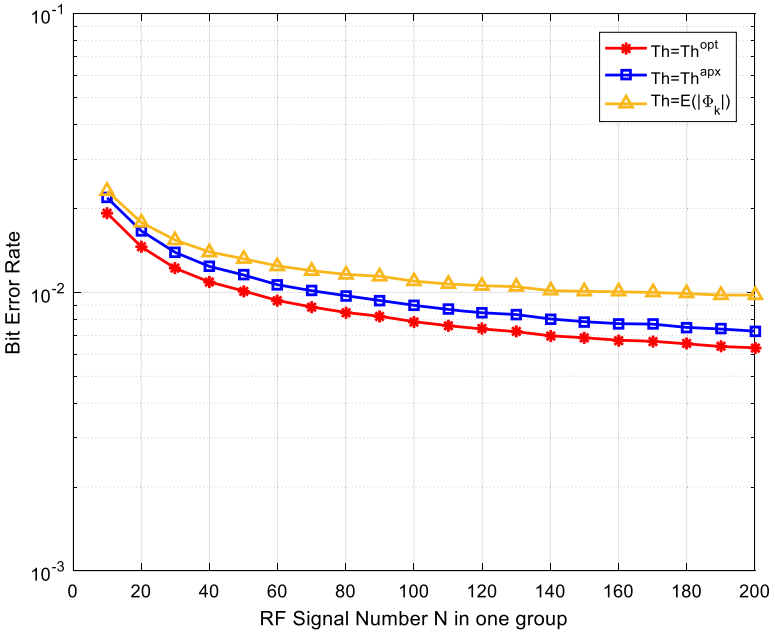


**Fig. 7.** BER versus signal number $N$ of RF signals in one group.

## 6 Conclusion

In this paper, we study the signal detection of ambient backscatter communication. Differential encoding model is used at the tag to help the reader implement signal detection. Based on the existing detecting threshold, we do more analysis and propose optimal thresholds decision algorithm. We also find the scenario where this algorithm has the best applicability and improves system performance greatly. Furthermore, we derive BER expressions to connect BER with parameters in the system model. Finally, simulation results are provided to corroborate our theoretical results. The results show that our proposed optimal thresholds decision algorithm will improve system performance to some extent, such as detection accuracy, transmitting distance and complexity, especially when the channel status are poor.

## Appendix

The function $p_1(x)$ is expressed as (17) shows. It is the sum of two PDFs of Gaussian random variables whose mean is $\delta$ and $-\delta$ respectively and they have the same variance:$\varsigma_+^2$. Derive function $p_1(x)$ and assume $\frac{dp_1(x)}{dx} = 0$, we will get

$$e\frac{2x\delta}{\varsigma_+^2} = \frac{\delta + x}{\delta - x}. \tag{A.1}$$

Since $p_1(x)$ is symmetry about y axis so we just discuss its properties in $(0, +\infty)$, and whatever $\delta$ is positive or negative, the result will be the same, so here we just take $\delta > 0$ into consideration.

The term on the left hand side of the equation is always positive in $(0, +\infty)$, so to make the equation work, there must be $x < \delta$. After deforming the above equation further, we obtain

$$e\frac{2x\delta}{\varsigma_+^2} = \frac{2\delta}{\delta - x} - 1. \tag{A.2}$$

Define

$$a_1(x) = e\frac{2x\delta}{\varsigma_+^2}, a_2(x) = \frac{2\delta}{\delta - x} - 1, \tag{A.3}$$

they are exponential function and negative power function, respectively. Observing (A.2) and we find that $x = 0$ is an absolute solution, which means that there will be a peak at $x = 0$. The appearance of another peak lies in whether another intersection point of two functions exists. When $x \to \delta, a_1(x) \to e\frac{2\delta^2}{\varsigma_+^2}, a_2(x) \to +\infty$, so to find the intersection point, we analyze the trend of them. We obtain the derivation at $x = 0$, when $\frac{da_1(x)}{dx}|_{x=0} > \frac{da_2(x)}{dx}|_{x=0}$, there must be another intersection point for two functions

and its value is smaller than $\delta$. In contrast, when $\frac{da_1(x)}{dx}|_{x=0} < \frac{da_2(x)}{dx}|_{x=0}$,$a_1(x)$ will never exceed $a_2(x)$ in $(0, \delta)$ and they will not meet in $(0, +\infty)$.

The derivations are shown as follows

$$\frac{da_1(x)}{dx}|_{x=0} = \frac{2\delta}{\varsigma_+^2}, \frac{da_2(x)}{dx}|_{x=0} = \frac{2\delta}{\delta^2}. \tag{A.4}$$

Thus we can get the conclusion: when $\delta > \varsigma_+$, function $p_1(x)$ has two peaks and it only has one peak when $\delta < \varsigma_+$.

## References


1. Xie, L., Yin, Y., Vasilakos, A.V., Lu, S.: Managing RFID data: challenges, opportunities and solutions. IEEE Commun. Surv. Tutor. **16**(3), 1294–1311 (2014)
2. Dobkin, D.M.: The RF in RFID: Passive UHF RFID in Pratice. Newnes (Elsevier), Oxford (2008)
3. Stockman, H.: Communication by means of reflected power. IRE **36**, 1196–1204 (1948)
4. Griffin, J.D., Durgin, G.D.: Gains for RF tags using multiple antennas. IEEE Trans. Antennas Propag. **56**(2), 563–570 (2008)
5. Boyer, C., Roy, S.: Backscatter communication and RFID: coding, energy and MIMO analysis. IEEE Trans. Commun. **62**(3), 770–785 (2014)
6. Griffin, J.D., Durgin, G.D.: Complete link budgets for backscatter radio and RFID systems. IEEE Antennas Propag. Mag. **51**(2), 11–25 (2009)
7. Griffin, J.D., Durgin, G.D.: Multipath fading measurements at 5.8 GHz for backscatter tags with multiple antennas. IEEE Trans. Antennas Propag. **58**(11), 3694–3700 (2010)
8. Kimionis, J., Bletsas, A., Sahalos, J.N.: Increased range bistatic scatter radio. IEEE Trans. Commun. **62**(3), 1091–1104 (2014)
9. Liu, V., Parks, A., Talla, V., Gollakota, S., Wetherall, D., Smith, J.R.: Ambient backscatter: wireless communication out of thin air. In: Proceedings of the ACM SIGCOMM, Hong Kong, China, pp. 1–13 (2013)
10. Qian, J., Gao, F., Wang, G.: Signal detection of ambient backscatter system with differential modulation. In: 2016 IEEE International Conference on Acoustics, Speech and Signal Processing (ICASSP), Shanghai, pp. 3831–3835 (2016)
11. Qian, J., Gao, F., Wang, G., Jin, S., Zhu, H.: Noncoherent detections for ambient backscatter system. IEEE Trans. Wirel. Commun. **16**(3), 1412–1422 (2017)
12. Wang, G., Gao, F., Fan, R., Tellambura, C.: Ambient backscatter communication systems: detection and performance analysis. IEEE Trans. Commun. **64**(11), 4836–4846 (2016)
13. Dong, M., Tong, L.: Optimal design and placement of pilot symbols for channel estimation. IEEE Trans. Signal Process. **50**(12), 3055–3069 (2002)
14. Xing, C., Ma, S., Zhou, Y.: Matrix-monotonic optimization for MIMO systems. IEEE Trans. Signal Process. **63**(2), 334–348 (2015)
15. Mat, Z., Zeng, T., Wang, G., Gao, F.: Signal detection for ambient backscatter system with multiple receiving antennas. In: Proceedings of the IEEE 14th Canadian Workshop on Information Theory (CWIT), St. John's, NF, Canada, July 2015, pp. 1–4 (2015)

16. Zhang, Y., Qian, J., Gao, F., Wang, G.: Outage probability for ambient backscatter system with real source. In: 2017 IEEE 18th International Workshop on Signal Processing Advances in Wireless Communications (SPAWC), Sapporo, pp. 1–5 (2017). https://doi.org/10.1109/spawc.2017.8227638
17. Wang, G., Gao, F., Dou, Z., Tellambura, C.: Uplink detection and BER analysis for ambient backscatter communication systems. In: Proceedings of the IEEE Global Communications Conference (GLOBECOM), December 2015, pp. 1–6 (2015)
18. Kellogg, B., Talla, V., Gollakota, S., Smith, J.R.: Passive Wi-Fi: bringing low power to Wi-Fi transmissions. In: Proceedings of the 13th USENIX Symposium on Networked Systems Design and Implementation (NSDI), Santa Clara, CA, USA, pp. 1–14 (2016)